Targeting HSP90 with the small molecule inhibitor AUY922 (luminespib) as a treatment strategy against hepatocellular carcinoma

Giuseppa Augello[1], Maria Rita Emma[1], Antonella Cusimano[1], Antonina Azzolina[1], Sarah Mongiovì[1], Roberto Puleio[2], Giovanni Cassata[2], Alessandro Gulino[3], Beatrice Belmonte[3], Roberto Gramignoli[4], Stephen C. Strom[4], James A. McCubrey[5], Giuseppe Montalto[1,6] and Melchiorre Cervello [1]

[1]Institute of Biomedicine and Molecular Immunology "Alberto Monroy", National Research Council (CNR), Palermo, Italy
[2]Istituto Zooprofilattico Sperimentale della Sicilia "A. Mirri", Histopathology and Immunohistochemistry Laboratory, Palermo, Italy
[3]Tumor Immunology Unit, Department of Health Science, University of Palermo, Palermo, Italy
[4]Division of Pathology, Department of Laboratory Medicine, Karolinska Institutet, Stockholm, Sweden
[5]Department of Microbiology and Immunology, Brody School of Medicine at East Carolina University, Greenville, North Carolina, USA
[6]Biomedic Department of Internal Medicine and Specialties, University of Palermo, Palermo, Italy

Hepatocellular carcinoma (HCC) is a highly malignant tumor that responds very poorly to existing therapies, most probably due to its extraordinary inter- and intra-tumor molecular heterogeneity. The modest therapeutic response to molecular targeted agents underlines the need for new therapeutic approaches for HCC. In our study, we took advantage of well-characterized human HCC cell lines, differing in transcriptomic subtypes, DNA mutation and amplification alterations, reflecting the heterogeneity of primary HCCs, to provide a preclinical evaluation of the specific heat shock protein 90 (HSP90) inhibitor AUY922 (luminespib). Indeed, HSP90 is highly expressed in different tumor types, but its role in hepatocarcinogenesis remains unclear. Here, we analyzed HSP90 expression in primary human HCC tissues and evaluated the antitumor effects of AUY922 *in vitro* as well as *in vivo*. HSP90 expression was significantly higher in HCC tissues than in cirrhotic peritumoral liver tissues. AUY922 treatment reduced the cell proliferation and viability of HCC cells in a dose-dependent manner, but did not do so for normal human primary hepatocytes. AUY922 treatment led to the upregulation of HSP70 and the simultaneous depletion of HSP90 client proteins. In addition, in a cell type-dependent manner, treatment induced either both caspase-dependent β-catenin cleavage and the upregulation of p53, or Mcl-1 expression, or *NUPR1* expression, which contributed to the increased efficacy of, or resistance to, treatment. Finally, *in vivo* AUY922 inhibited tumor growth in a xenograft model. In conclusion, HSP90 is a promising therapeutic target in HCC, and AUY922 could be a drug candidate for its treatment.

Introduction

Hepatocellular carcinoma (HCC) is the third leading cause of cancer-related mortality worldwide.[1] Although, the treatment of patients with HCC has improved considerably in recent

years, unfortunately, in many cases, diagnosis is not made until the disease is at an advanced stage when curative therapies, such as liver resection, liver transplantation or local ablation, cannot be used.

Sorafenib is an oral multikinase inhibitor which targets Raf kinases, vascular endothelial growth factor (VEGFR)-2/-3, platelet-derived growth factor receptor β (PGFR-β), c-Kit proto-oncogene receptor tyrosine kinase and Fms-like tyrosine kinase 3 (Flt-3).[2] It is the only approved drug for treating advanced HCC.[3] However, its efficacy is limited, and drug resistance remains a major obstacle to improving survival rates.[3] Other drugs acting on different signaling pathways involved in HCC have given disappointing results,[2] emphasizing the need to develop new and more specific therapeutic approaches.

HCC is characterized by extraordinary inter- and intra-tumor molecular heterogeneity,[4–7] which is probably responsible for the modest therapeutic response to molecular targeted agents. Future studies should aim at better characterizing and stratifying HCC patients into subgroups, according to their molecular profiles, in order to benefit from treatment with

What's new?

Hepatocellular carcinoma (HCC) exhibits vast molecular heterogeneity, suggesting that therapies aimed against targets that interact with multiple signaling pathways could be key to improving HCC outcome. Here, heat shock protein 90 (HSP90), a modulator of numerous signaling components, was found to be highly expressed in HCC. AUY922, an HSP90 inhibitor, blocked HCC cell growth *in vitro* and, in HepG2 liver carcinoma cells, induced apoptosis via caspase activation and β-catenin fragmentation. These effects were not observed in Huh7 or SNU475 HCC cell lines. AUY922 also reduced tumor growth *in vivo*, marking HSP90 as a promising therapeutic target in HCC.

single molecular targeted agents or combinations of them under the heterogeneous conditions of HCC tumors.[4,8]

In consideration of the complexity of HCC, targeting a single component of a signaling pathway may be ineffective. Therefore, a good molecular target is one that modulates many components of one or more signaling pathways at the same time. Heat shock protein 90 (HSP90) is one of the most important molecular chaperones, and hundreds of proteins that interact with it, referred to as client proteins, have been identified to date.[9] HSP90 regulates the stability, function and activity of numerous oncoproteins, thus contributing to the malignant phenotype. Among others, oncogenic client proteins of HSP90 are implicated in cell growth and proliferation (AKT, EGFR, β-catenin), apoptosis (p53, AKT) and angiogenesis (VEGFR). Most of these proteins are very commonly dysregulated in HCC,[2] so HSP90 may represent an attractive therapeutic target in HCC.[10] HSP90 is highly expressed in different tumor types,[11] but its role in hepatocarcinogenesis remains unclear.

Given the key role of HSP90 in the control of oncogenic signals, many pharmaceutical companies have recently developed a variety of small molecule inhibitors which are selective for HSP90. Several studies have shown that AUY922 (luminespib), a potent third-generation HSP90 inhibitor, has antitumor activity in a wide range of human cancer cells.[12–16] AUY922 is a resorcinylic isoxazole amide that inhibits the ATPase activity of HSP90. AUY922 is currently being tested in several phase II clinical studies of different cancer types[9] (NCT01389583; NCT01854034; NCT01752400). However, to date, there have been no studies of AUY922 administration in HCC.

Cancer cell lines are valuable *in vitro* models for analyzing genetic heterogeneity within tumors and for screening pharmacologic agents for anticancer assessment.[17,18] Recently, on the basis of transcriptome meta-analysis of 603 clinical HCC tissues, HCC cell lines have been classified into subtypes.[18,19] Interestingly, each subtype demonstrated a different sensitivity to molecular target agents,[18–22] with the so-called S1-like cells, such as SNU475, SNU387 and SNU182, showing more susceptibility to the Src/Abl inhibitor dasatinib,[20] whereas S2-like cell lines, such as HepG2, Huh7, Hep3B and PLC/PRF/5, showed higher sensitivity to JQ1, a bromodomain inhibitor targeting the Myc pathway,[18] or to BJC398, a fibroblast growth factor receptor (FGFR) inhibitor,[19] or to epidermal growth factor receptor (EGFR) and insulin-like growth factor receptor (IGF1R) inhibitors;[21,22] these results highlight the

invaluable resource offered by cancer cell lines as experimental models for antitumor agent development and assessment.

In the present study, we used HCC cells expressing different transcriptomic subtypes and endowed with different DNA mutation/amplification alterations, reflecting the heterogeneity of primary HCCs,[18] to provide an *in vitro* and *in vivo* preclinical evaluation of AUY922 antitumor effects in HCC and to explore the mechanism responsible of different sensitivity of HCCs to drug treatment.

Materials and Methods
Reagents and antibodies
The reagents and antibodies used are listed in Supporting Information Table S1.

Tissue specimens and immunohistochemistry
The study included 12 paired primary HCC patients whose surrounding peritumoral regions (cirrhotic tissues) showed hepatitis virus B (HBV)-associated (n = 1) or HCV-associated (n = 11) chronic liver disease (6 male, 6 females; mean age 67.6, range 42–82 years). Normal liver biopsies were obtained from patients undergoing surgical operations for cholecystectomy. Patients' primary clinical characteristics are reported in Supporting Information Table S2. All patients had undergone surgery at the University of Palermo Medical School (Italy). Informed consent was obtained from all patients. The study protocol was conformed to the ethical guidelines of the 1975 Declaration of Helsinki.

Immunohistochemical analyses were performed as previously reported.[23] Two independent pathologists (AG and BB) evaluated the relative percentages of positive cells, as well as staining intensity. Staining intensity was scored as follows: 0 (no staining), 1 (weak), 2 (moderate) and 3 (strong). Percentages of positive cells were scored as follows: 0 (no positive cells), 1 (1–25% positive), 2 (26–50% positive), and 3 (>50% positive). The two scores were added together to give a single score, from 0 to 6.

Cell cultures
HepG2, Hep3B and SNU475 cells were purchased from the American Type Culture Collection (Rockville, MD). PLC/PRF/5 and Huh7 cells were a gift from Professor O. Bussolati (University of Parma, Italy) and Professor M. Levrero (Sapienza University of Rome, Italy), respectively.

All cell lines were authenticated by short tandem repeat (STR) profiling (BMR Genomics, Padua, Italy) and used within 6 months of receipt. Cells were maintained as previously reported.[24] Normal human primary hepatocytes were isolated and cultured as previously reported.[25]

Cell viability, proliferation assays and evaluation of caspase 3/7 activity

Cells were seeded in 96-well plates and, after 24 h, were exposed to AUY922 alone or in combination with sorafenib. After treatment, cell viability, cell proliferation and caspase 3/7 activity were measured as previously reported.[25,26] All data shown are the mean ± standard deviation (SD) from three experiments performed in triplicate.

Western blotting

Immunoblotting was performed as previously reported.[27] The relative expressions were calculated as the ratio of drug-treated samples *vs.* control (dimethylsulfoxide, DMSO) and corrected using the quantified level of β-actin expression. The data shown are representative of three independent experiments with comparable results.

Immunofluorescence, cell transfection, RNA extraction, real-time polymerase chain reaction (PCR) and β-catenin transcriptional activity

Immunofluorescence analysis and cell transfection with specific nuclear protein 1 (NUPR1) and Mcl-1 small interference RNAs (siRNAs) (Supporting Information Table S1) were performed as previously reported.[23,28] Briefly, for immunofluorescence analysis, HCC cells were seeded in chamber slides and, after 24 h, treated with 100 nM of AUY922 for another 24 h. Cells were fixed, permeabilized and stained with primary anti-NUPR1 antibody. After staining, slides were mounted with Vectashield mounting medium containing DAPI (Vector Laboratories Inc., Peterborough, UK) to visualize cell nuclei. Images were acquired with a Leica microscope.

For siRNA transfection, 3.5×10^5 Huh7 cells and 2.0×10^5 of SNU475 cells were seeded in 6-well plates. After 24 h, 50 nmol/l of Mcl-1 siRNA or NUPR1 siRNA (siMcl-1 and siNUPR1) were used. Control cell transfection was performed with a Negative Control siRNA (siNC). Cell transfections were carried out with Lipofectamine RNAiMax (Invitrogen, Carlsbad, CA, USA), following the manufacturer's instructions. Cells were detached after 24 h of transfection and seeded in 96-well plates or 60-mm plates for MTS assay or protein extraction, respectively.

After 24 h of transfection, a cell viability assay, RNA extraction and quantitative Real-Time PCR were performed as previously reported.[23] Briefly, total RNA was extracted from cells using TRIzol reagent, and 1 μg of RNA was used for reverse transcription to generate cDNA. Expression of selected genes was quantified by QuantiNova SYBR Green fluorescence Real-Time PCR (Qiagen, Milan, Italy), using specific primers (Supporting Information Table S1). Real Time PCR data were

expressed as the relative mRNA expression level of the different genes in treated cells compared to control cells. Values given are the mean ± SD of three different experiments performed in triplicate. Semiquantitative PCR was performed using specific primers (Supporting Information Table S1). The cycling conditions were conducted using the following program: for survivin, 94 °C (5 min), then 94 °C (30 s), 60 °C (30 s); for cyclin D1, 94 °C (5 min), then 94 °C (30 s), 58 °C (30 s); for β- actin, 60 °C (30 s), then 72 °C (30 s), and a final elongation step at 72 °C (10 min). Electrophoresis on agarose gel was performed to analyze amplified PCR products.

β-catenin transcriptional activity was measured using the TOPflash/FOPflash luciferase system as previously reported.[29]

In vivo studies

Female athymic nude mice (Fox1 nu/nu) (4 weeks of age; 6 mice/group) were purchased from Envigo (Udine, Italy). All procedures were conducted according to institutional guidelines which were conformed to national and international laws and policies. The study was authorized by the Italian Ministry of Health (no. 1187/2015-PR). Animals were subcutaneously inoculated with 10×10^6 Huh7 cells. AUY922 was dissolved in 5% 2-hydroxypropyl-β-cyclodextrin at 1 mg/ml concentration. When tumors were palpable (approximately 150 mm^3), the mice were randomly assigned to two groups; the control group (C) received the vehicle alone (10% DMSO, 5% Tween 20 and 85% saline), and the treated group (T) received 30 mg/kg of AUY922 by intra-peritoneal injection five times a week for 15 days. Tumor volumes and body weight measurements were performed as previously reported,[30] and the data obtained were presented as mean ± standard error (SE). Western blotting and immunohistochemistry analyses were performed as previously reported.[30]

Statistical analysis

Statistical analysis was performed using Student's t-test (two-tailed). The Mann Whitney test was used for analyzing immunohistochemistry results. The criterion for statistical significance was $p < 0.05$. For the synergistic activity, data were analyzed using CalcuSyn software v. 2.0 (Biosoft, Cambridge, UK), in which CI < 1 indicated synergy, ~1 indicated an additivity and >1 indicated antagonism. IC$_{50}$ was calculated using the GraphPad Prism 6 software (GraphPad Software, La Jolla, CA, USA) by linear regression.

Results

HSP90 expression in HCC tissues and cirrhotic peritumoral liver tissues

To explore the clinical relevance of HSP90 in liver cancer, its expression was assessed by immunohistochemistry in 12 pairs of human liver cirrhosis-associated HCC tissues and their corresponding adjacent non-cancerous liver tissues, as well as in 3 normal liver (NL) tissues (Fig. 1*a*). Immunohistochemical analysis showed significantly higher HSP90 expression in HCC tissues (T) than in cirrhotic peritumoral tissues (P) ($p < 0.01$).
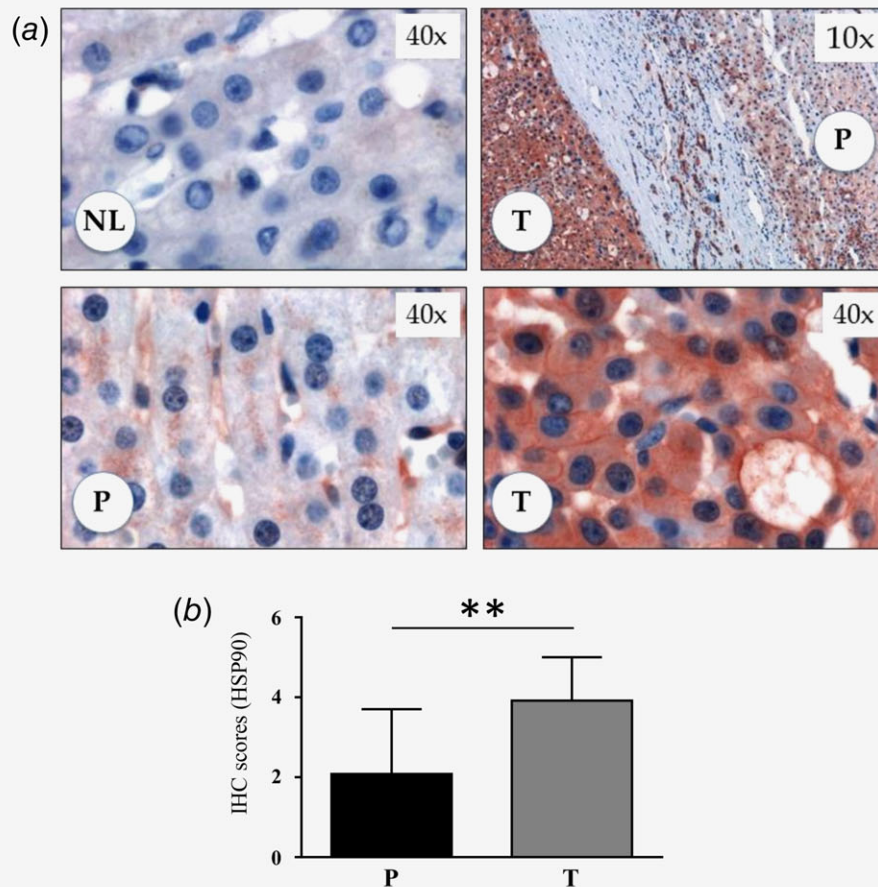
Figure 1. HSP90 expression in primary human HCC samples. (*a*) HSP90 protein expression levels were examined by immunohistochemistry in normal liver (NL) and HCC tissues. Peritumoral tissue (P) and tumoral tissue (T) are shown. Magnification is indicated. (*b*) Immunohistochemistry scores in P and T tissues. ** *p* < 0.01. [Color figure can be viewed at wileyonlinelibrary.com]

The sum of the scores (intensity + percentage of positive cells) for HSP90 expression was significantly higher in HCC tissues (3.91 ± 1.08) compared to cirrhotic peritumoral liver tissues (2.08 ± 1.62) ($p < 0.01$) (Fig. 1*b* and Supporting Information Table S3).

AUY922 reduced the viability and proliferation of HCC cells, but not of normal hepatocytes, and inhibited HSP90 activity

The basal expression level of HSP90 protein was analyzed in five human HCC cell lines, HepG2, Huh7, Hep3B, PLC/PRF/5 and SNU475, all of which expressed HSP90, though each showed a different expression level (Fig. 2*a*).

The effect of AUY922 on cell viability was measured by MTS assay. As shown in Figure 2*b*, AUY922 reduced cell viability in a dose- and time-dependent manner in four of five HCC cell lines (Fig. 2*b*), but it showed no cytotoxicity in normal human primary hepatocytes (Fig. 2*c*). The 50% inhibitory concentration (IC_{50}) values ranged from 9.2 to 16.2 μM in Huh7 and Hep3B cells, respectively, at 72 h (Supporting Information Table S4), whereas a minimal effect on SNU475 cells was observed, even at the highest dose tested (200 nM).

Based on these results, we selected HepG2, Huh7 and SNU475 cells as models for all subsequent experiments, with HepG2 and Huh7 cells being the most responsive and SNU475 the most resistant to AUY922 treatment. However, HSP90 activity was inhibited similarly in the three HCC cell lines, as demonstrated by the upregulation of HSP70 (Fig. 2*d*). This effect has been shown to be due to the dissociation of heat shock factor 1 (HSF1) monomer from HSP90, with subsequent HSF1 trimerization, nuclear translocation and transcriptional activation of genes coding for heat shock proteins, including HSP70.[31] Therefore, HSP70 upregulation is considered one of the hallmarks of HSP90 inhibition, along with the downregulation of HSP90 clients, such as AKT, ERK and EGFR (Fig. 2*d*). In addition, AUY922 inhibited the activation of AKT and ERK signaling, as highlighted by decreased phosphorylated forms of these kinases (Fig. 2*d*). Due to their role in controlling cell proliferation, the ability of AUY922 to inhibit HCC cell proliferation was evaluated by BrdU assays. As expected, a dose-dependent inhibitory effect on cell proliferation in the three cell lines was observed (Fig. 2*e*).
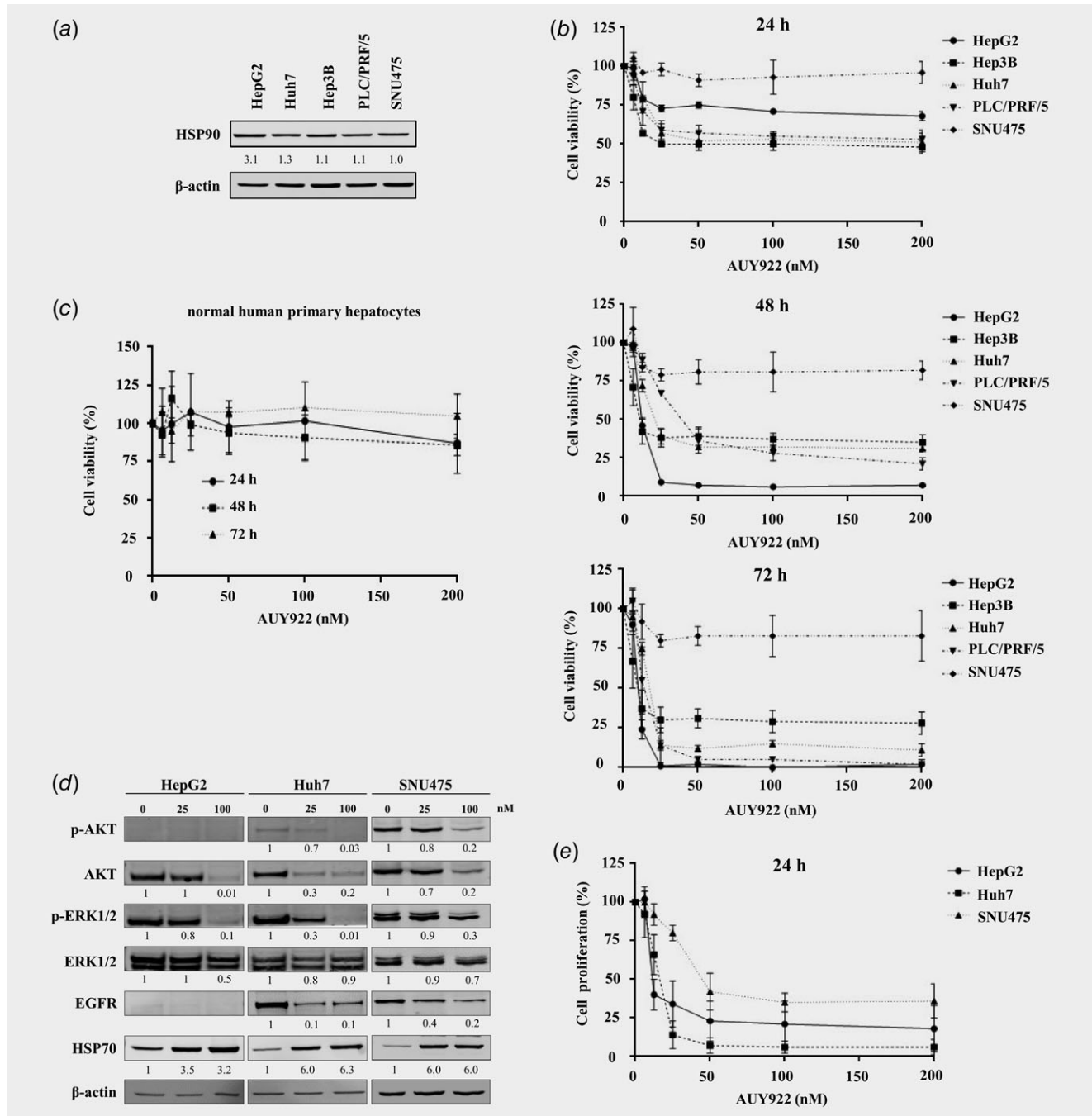
Figure 2. Expression of HSP90 and HSP90-client proteins in HCC cells, cell viability and proliferation in HCC cell lines and normal human primary hepatocytes. (*a*) Immunoblotting evaluation of HSP90 expression in HCC cells. (*b*) HCC cells were treated with AUY922 at the indicated concentrations for 24–48-72 h, and cell viability was evaluated by MTS assays. (*c*) Normal human primary hepatocytes were treated with AUY922 at the indicated concentrations for 24–48-72 h, and cell viability was evaluated by Cell Titer-Glo® assays. (*d*) Immunoblotting evaluation of p-AKT, AKT, p-ERK1/2, ERK1/2, EGFR and HSP70 expression in HCC cells. (*e*) HCC cells were treated with AUY922 at the indicated concentrations for 24 h, and cell proliferation was evaluated by BrdU incorporation into DNA.

AUY922 triggered apoptosis *via* activation of caspases, fragmentation of β-catenin and inhibition of β-catenin-mediated transcriptional activity in HepG2 cells

Apoptosis induction was investigated by analyzing poly(-ADPribose) polymerase 1 (PARP) cleavage and the expression of the tumor suppressor p53 and anti-apoptotic proteins Bcl-2 and Mcl-1, and by measuring the activation of caspase-3/7.

AUY922 treatment induced PARP cleavage in HepG2 cells, suggesting the activation of caspase cascade, but not in Huh7 or SNU475 cells (Fig. 3*a*). Accordingly, an increase in caspase-3/7
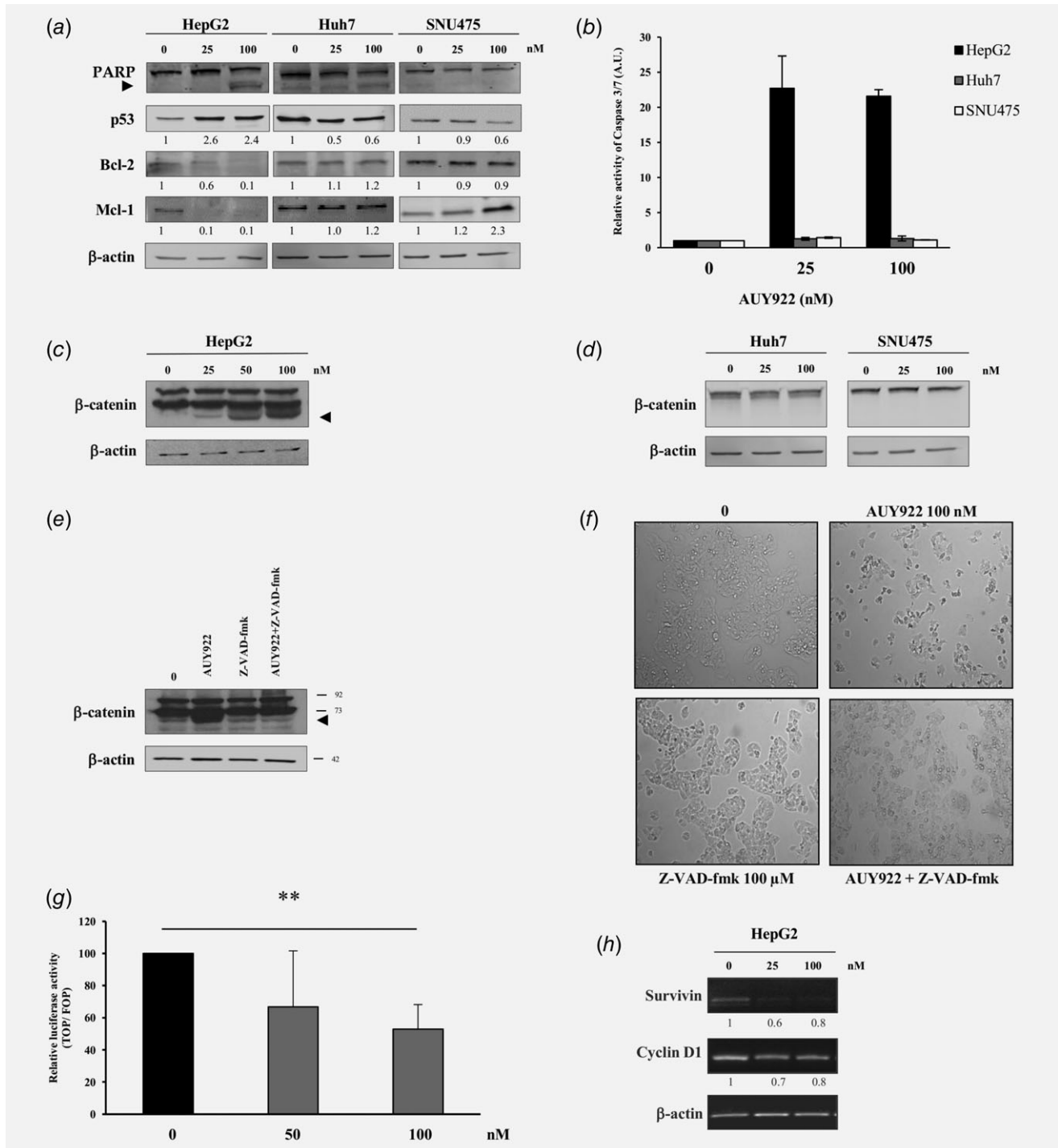
Figure 3. AUY922 induced apoptosis and inhibited β-catenin transcriptional activity in a cell-type dependent manner in HCC cells. (*a*) Immunoblotting evaluation of apoptosis-related protein expression in HCC cells. The PARP fragment (85 kDa) is indicated by an arrowhead. (*b*) Caspase-3/7 activity levels in HCC cells after AUY922 treatment at the indicated concentrations for 24 h. Data are given as Arbitrary Units (A.U.) normalized to control values. (*c*,*d*) Representative Western blotting analysis of β-catenin expression in HCC cells after AUY922 treatment for 24 h. The β-catenin fragment is indicated by an arrowhead. (*e*) Western blotting analysis of β-catenin expression after treatment of HepG2 cells with 100 nM AUY922 and/or 100 μM z-VAD-fmk for 24 h. (*f*) HepG2 cell morphology after treatment with AUY922 and/or z-VAD-fmk for 24 h. (*g*) β-catenin transcriptional activity in HepG2 cells treated with AUY922. Cells were transfected with pTOPflash or pFOPflash constructs, and 24 h later, the cells were treated with AUY922 for 24 h. Data are expressed as TOPflash/FOPflash ratio and normalized to the activity of a co-transfected ß-galactosidase plasmid in the same experiment. **p < 0.01, 100 nM AUY922 *vs*. control. (*h*) Survivin and cyclin D1 mRNA levels were evaluated by semi-quantitative RT-PCR after treatment of HepG2 cells with AUY922 for 24 h. The results shown are in the linear range of PCR amplification.

activity was observed in HepG2 cells, but not in Huh7 or SNU475 cells (Fig. 3b); p53 expression was unchanged after treatment in Huh7 and SNU475 cells, whereas in HepG2 cells increased protein expression was observed (Fig. 3a). Moreover, downregulation of Bcl-2 expression was observed only in HepG2 cells, whereas an increase of Mcl-1 was observed in SNU475 cells, but not in HepG2 or Huh7 cells (Fig. 3a). These results suggest that each cell line behaved differently after treatment with AUY922.

β-catenin is an HSP90 client protein, and some apoptotic stimuli can induce caspase-dependent cleavage of β-catenin in HCC cells.[28,29] As shown in Figure 3c, AUY922 treatment triggered β-catenin cleavage in HepG2 cells, but not in Huh7 or SNU475 cells (Fig. 3d). β-catenin cleavage was inhibited by the co-administration of the pan-caspase inhibitor z-VAD-fmk with AUY922 (Fig. 3e), confirming caspase involvement. In addition, after AUY922 treatment in combination with z-VAD-fmk, a clear recovery of cell morphology was observed, with reduced cell shrinkage and detachment (Fig. 3f). Moreover, AUY922-induced fragmentation of β-catenin in HepG2 cells resulted in the inhibition of β-catenin-mediated transcriptional activity as measured by gene reporter assay (Fig. 3g) and the reduced expression of β-catenin target genes coding for survivin and cyclin D1 (Fig. 3h).

Mcl-1 was responsible for the sensitizing effect of AUY922 in SNU475 cells

Western blotting analysis revealed that the expression of the anti-apoptotic protein Mcl-1 increased after AUY922 administration in SNU475 cells, but not in HepG2 or Huh7 cells (Fig. 3a). This observation led us to evaluate the functional role of Mcl-1 in the apoptotic resistance of SNU475 cells to AUY922, especially in consideration of the key role of Mcl-1 in HCC chemoresistance.[28,32] Therefore, HCC cells were transfected with Mcl-1-specific siRNA to inhibit *Mcl-1* gene expression. Transfection efficiency after 72 h of transfection with siMcl-1 was confirmed by a clear reduction in Mcl-1 protein expression levels (Fig. 4a). Mcl-1 knockdown (KD) significantly sensitized SNU475 cells to AUY922 treatment, reducing cell viability (Fig. 4b) and promoting AUY922-induced PARP cleavage (Fig. 4c).

NUPR1 was responsible for the sensitizing effect of AUY922 in Huh7 cells

We have recently demonstrated that the overexpression of NUPR1, a stress inducible protein, plays an essential role in the survival and chemoresistance of HCC cells.[23,28] Therefore, expression levels of NUPR1 mRNA and protein were also investigated. AUY922 treatment increased NUPR1 mRNA and protein expression in Huh7 cells (Fig. 4d, e), but not in HepG2 or SNU475 cells. Therefore, we examined whether the inhibition of *NUPR1* could affect the sensitivity of Huh7 cells to AUY922. After evaluating transfection efficiency by Real-Time PCR of NUPR1 mRNA expression (Fig. 4f), the cell viability of transfected cells treated with AUY922 was measured. NUPR1 KD significantly sensitized Huh7 cells to AUY922 treatment, reducing cell viability (Fig. 4g) and promoting AUY922-induced PARP cleavage (Fig. 4h).

Combining AUY922 with sorafenib synergistically inhibited HCC cell viability

The observation that treatment with AUY922 altered ERK1/2 signaling prompted us to investigate the effect of combining AUY922 with the multi-kinase inhibitor sorafenib.[33] Treatment with 12.5 nM AUY922 in combination with different concentrations of sorafenib for 48 h effectively reduced cell viability in all cell lines (Fig. 5, left panels). According to the combination index (CI), the combination of 12.5 nM AUY922 with all concentrations of sorafenib resulted in synergistic effects in HepG2 and Huh7 cells (Fig. 5, right panels). For SNU475 cells, synergistic, additive or antagonistic effects were observed, depending of the combination used (Fig. 5, right panels).

### AUY922 treatment inhibited tumor growth *in vivo*

The potential therapeutic effects of AUY922 were tested *in vivo* using nude mice bearing HCC tumor xenografts. AUY922 treatment led to significantly reduced tumor volume compared to the vehicle alone (control group) (Fig. 6a). Moreover, mice treated with AUY922 did not show significantly altered body weight when compared to control group, suggesting that the treatment was well tolerated (Fig. 6b). In addition, HSP90 inhibition was associated with significantly increased HSP70 expression in post-treatment HCC samples (Fig. 6c), confirming that *in vivo* AUY922 inhibited HSP90 activity as demonstrated previously in *in vitro* experiments (Fig. 2d). Furthermore, immunohistochemical staining demonstrated that AUY922 treatment decreased cell proliferation and angiogenesis, as measured by the percentage of cells expressing the proliferation marker Ki67 (Fig. 6d) and the endothelial marker CD31 (Fig. 6e), respectively.

Discussion

HCC is one of the deadliest cancers, partly due to a lack of effective treatments. The failure of molecular targeted therapies is likely due to the intra- and inter-tumor molecular heterogeneity of HCC tumors resulting from different types of molecular aberrations, ultimately leading to patient-specific dysregulation of molecular pathways.[4–6,18]

In the present study, in accordance with data also reported by others,[34] we demonstrated that HSP90 expression was significantly higher in HCC tissues compared to cirrhotic peritumoral liver tissues, suggesting that high expression of HSP90 might be involved in the hepatocarcinogenesis process.

To study the functional role of HSP90 and evaluate the antitumor effects of HSP90 inhibitor AUY922, *in vitro* as well as *in vivo*, we used different HCC cell lines expressing different transcriptomic subtypes and endowed with different DNA mutation/amplification alterations, reflecting the heterogeneity
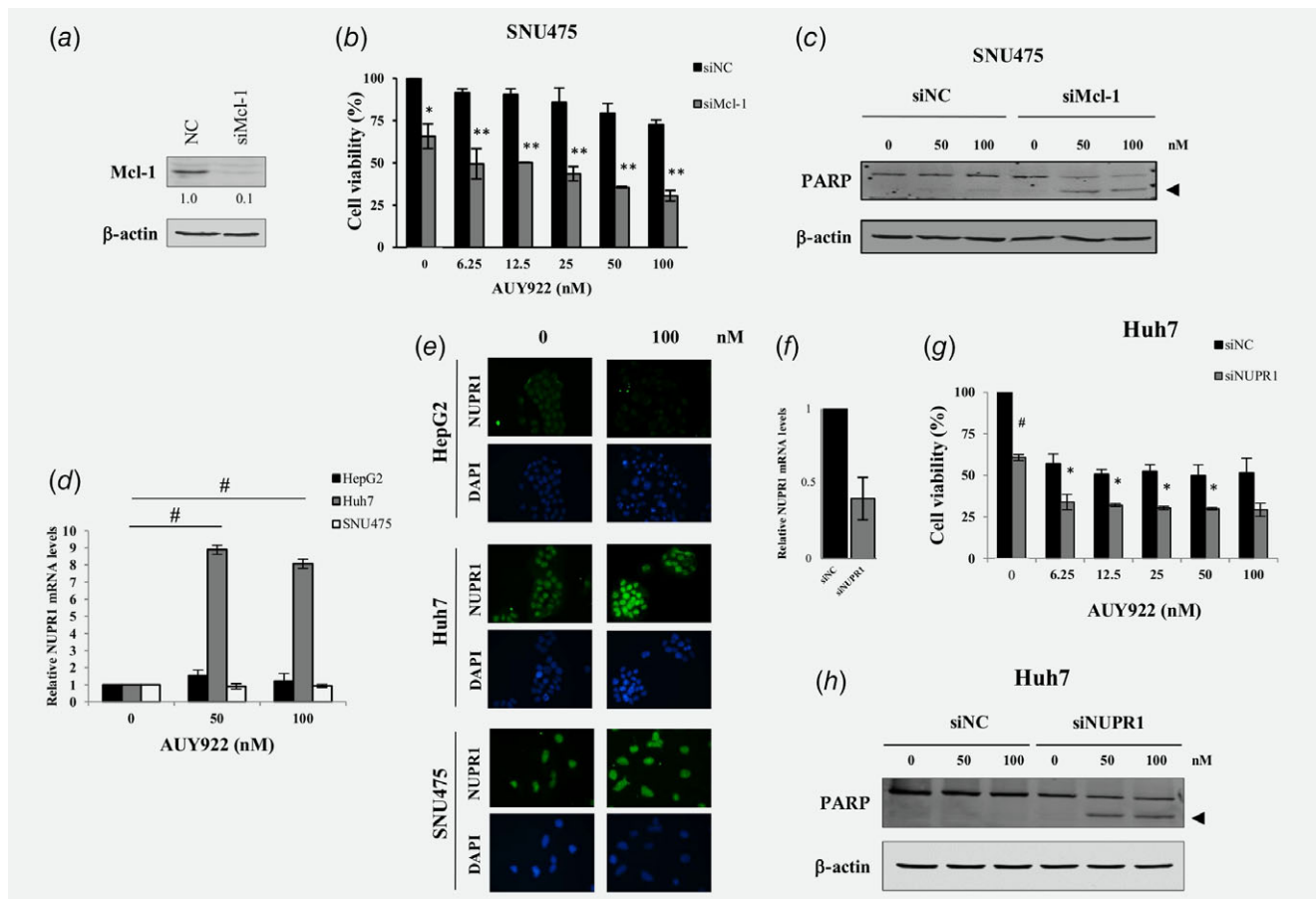
Figure 4. *Mcl-1* knockdown (KD) sensitized SNU475 cells to AUY922-mediated cell death and *NUPR1* KD sensitized Huh7 cells to AUY922-mediated cell death. (*a*) Western blotting analysis of Mcl-1 expression after 24 h of transfection with Mcl-1 siRNA (siMcl-1) compared to cells transfected with control siRNA (NC). (*b*) Cell viability of cells transfected with siMcl-1 after treatment with the indicated AUY922 concentrations for 24 h. *$p < 0.05$ siMcl-1 *vs.* siNC; **$p < 0.01$ siMcl-1 *vs.* siNC. (*c*) Western blotting analysis of PARP expression in cells transfected with siMcl-1 or siNC after 24 h of AUY922 treatment. The PARP fragment (85 kDa) is indicated by an arrowhead (*d*) Real-Time PCR of NUPR1 mRNA expression after AUY922 treatment of HCC cells for 24 h. #$p < 0.005$ AUY922 *vs.* control. (*e*) Immunofluorescence analysis of NUPR1 protein expression after treatment for 24 h with AUY922 in HCC cells. (*f*) Real-Time PCR of NUPR1 mRNA expression after 24 h of transfection with NUPR1 siRNA (siNUPR1) in Huh7 cells compared to cells transfected with control siRNA (NC). (*g*) Cell viability of cells transfected with siNUPR1 after treatment with the indicated AUY922 concentrations for 24 h. *$p < 0.05$ siNUPR1 *vs.* siNC; #$p < 0.005$ siNUPR1 *vs.* siNC. (*h*) Western blotting analysis of PARP expression in cells transfected with siNUPR1 or siNC after 24 h of AUY922 treatment. The PARP fragment (85 kDa) is indicated by an arrowhead. [Color figure can be viewed at wileyonlinelibrary.com]

of primary HCCs.[18] For example, HepG2 cells carry mutated *K-Ras* and *CTNNB1* (encoding for β-catenin), Hep3B cells are *p53*-null, Huh7, PLC/PRF/5 and SNU475 cells carry mutated *p53*, and PLC/PRF/5 cells carry mutant *K-Ras*. Interestingly, a recent study by Wang *et al.*[14] reported that AUY922 preferentially kills colon cancer cells carrying mutant *K-Ras*, which were also more prone to AUY922-induced ER stress. Accordingly, in the present study, cells with mutated *K-Ras*, such as HepG2 cells, were more prone to apoptosis induction compared to cells with wild-type *K-Ras*, such as Huh7 cells.

However, these results could also depend on the different p53 statuses in these two cell lines. The tumor suppressor p53 is an important HSP90 client protein and is mutated in over 50% of human cancers. It has been reported that HSP90 inhibition with the benzoquinone 17-dimethylaminoethylamino-

17-demethoxygeldanamycin (17-DMAG) induced apoptosis in a p53-dependent manner[35] and that blocking HSP90 activity with 17-allylamino-17-demethoxygeldanamycin (17-AAG) promoted the ubiquitination and degradation of mutated p53 *via* proteasome.[36] In our study, we demonstrated that AUY922 treatment triggered the downregulation of mut-p53 protein in Huh7 and SNU475 cells, whereas it promoted the upregulation of WT-p53 expression in HepG2 cells, leading to the activation of the apoptotic pathway, with PARP cleavage and increased caspase activity.

In addition, in HepG2 cells, the oncogenic Wnt signaling is constitutively activated, due to the deletion of exon 3 of the *CTNNB1* gene encoding β-catenin, whereby the activation of the Wnt/β-catenin pathway seems to be crucial for cell proliferation/survival of this cell type.[37] Here, we found that β-catenin
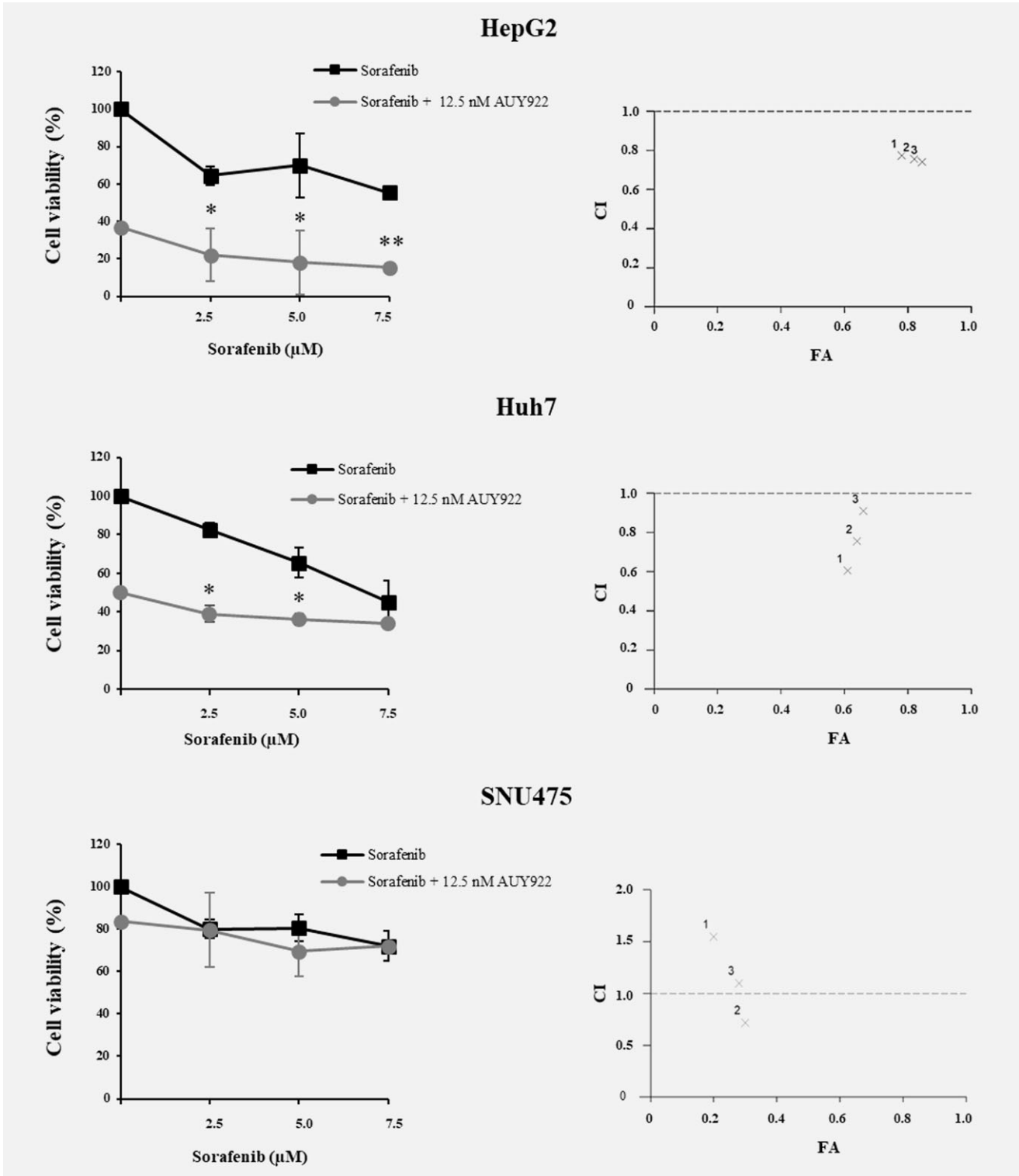
Figure 5. Treatment with AUY922 in combination with sorafenib synergistically inhibited cell viability in HCC cells. Left panels, viability of HCC cells treated with different doses of sorafenib combined with 12.5 nM AUY922 for 24 h. Right panels, the combined effect of sorafenib and AUY922 was evaluated using CalcuSyn software. CI-FA plots represent the combination index (CI) values and the fraction affected (FA) at different concentrations of sorafenib [(1) 2.5 μM; (2) 5 μM; (3) 7.5 μM] combined with 12.5 nM AUY922. CI < 1 indicates synergism between the two drugs. *p < 0.05, 12.5 nM AUY922 + sorafenib *vs.* 12.5 nM AUY922 alone; **p < 0.01, 10 nM AUY922 + sorafenib *vs.* 12.5 M AUY922 alone.
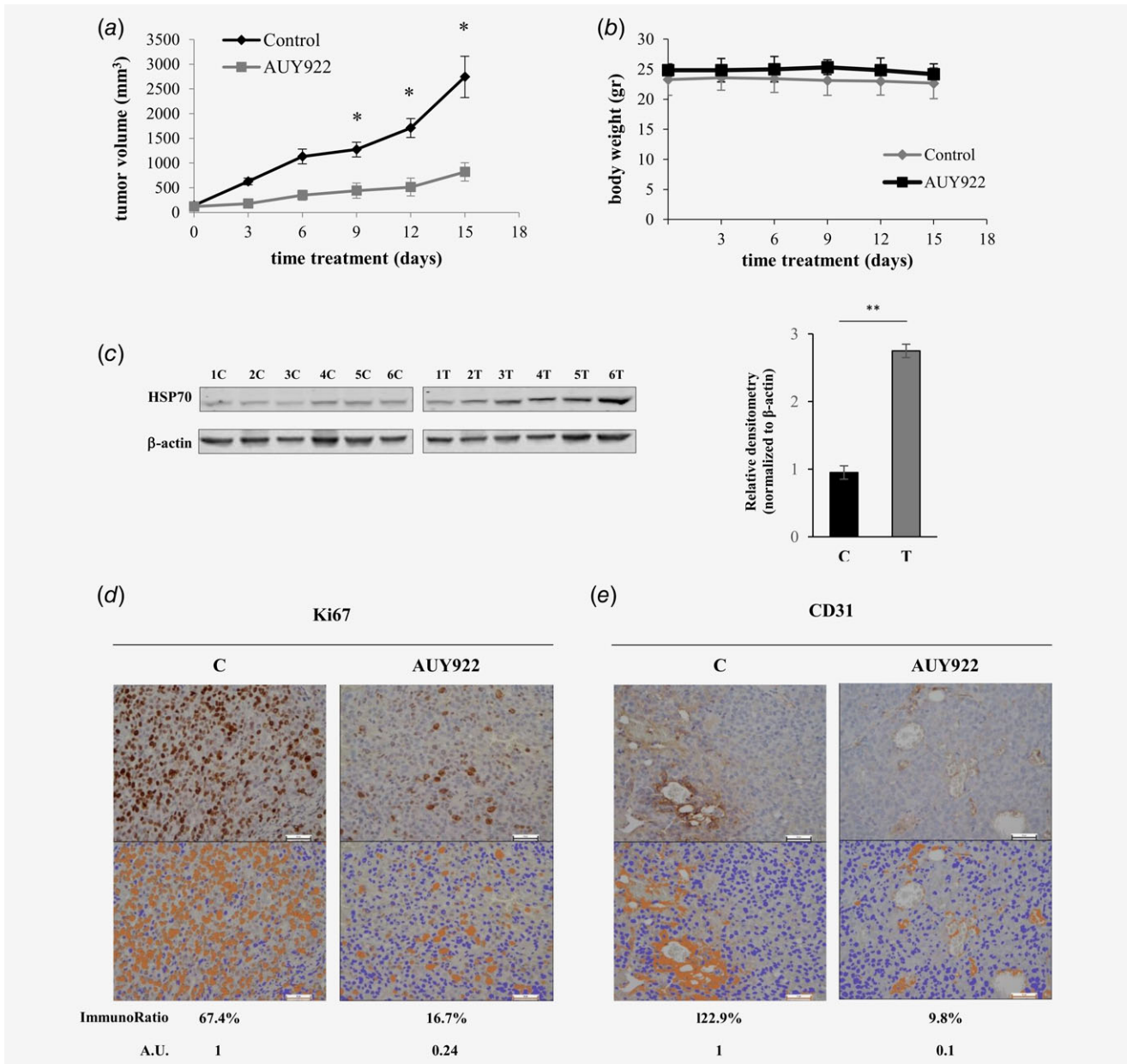
Figure 6. AUY922 inhibited tumor growth in xenograft models of Huh7 cells. (*a*) Tumor volume curve and (*b*) mice body weight alterations after treatment with 30 mg/kg AUY922. (*c*) Left panels, Western blotting showing HSP70 levels in control (C) and treated samples (T). Right panel, quantification of HSP70 expression. The numbers represent the median ± SD of HSP70 protein expression, after normalization with β-actin, with vehicle-treated control sample (C) arbitrarily set at 1.0. (*d,e*) Evaluation of Ki67 and CD31 expression by immunohistochemical staining in control and treated samples (AUY922) (scale bar = 50 μm). ImmunoRatio® software was used to quantify protein expression. Arbitrary Units (A.U.) normalized to control values. [Color figure can be viewed at wileyonlinelibrary.com]

was cleaved in a caspase-dependent manner, which in turn reduced β-catenin transcriptional activity with a consequent downregulation of cyclin D1 and survivin mRNA expression. Interestingly, the suppression of the β-catenin-cyclin D1 pathway, together with survivin reduction, has been shown to overcome AUY922 resistance in colorectal cancer cells.[38]

However, different modulators involved in resistance to HSP90 inhibitors have been investigated in colorectal cancer

and HCC cell lines.[39] Recently, Lee *et al.* have reported that the anti-apoptotic protein Mcl-1 plays a key role in sensitizing effects of AUY922 in colorectal cancer cells.[40] Here, we observed that AUY922 upregulated Mcl-1 expression in SNU475 cells. Furthermore, we demonstrated that the specific inhibition of Mcl-1 expression in SNU475 cells by siMcl-1 induced apoptosis in response to AUY922 treatment, thus suggesting that Mcl-1 expression could protect cells from

AUY922 antitumor effects. Therefore, our results provide a possible explanation of the mechanism of resistance to AUY922 treatment and might highlight the use of combinations of Mcl-1 small molecule inhibitors and AUY922 to improve therapeutic benefits in a subclass of HCC.

Previous studies have shown that HSP90 inhibition was associated with the ER stress response pathway.[14,41] It has been shown that the stress-associated protein NUPR1 mediates resistance to chemotherapy drugs,[42–44] as well as to molecular targeted agents.[23] Our results point to the important role of NUPR1 in resistance to AUY922 treatment. In support, NUPR1 silencing in Huh7 cells resulted in apoptosis induction upon AUY922 treatment, suggesting that, in a cell type-dependent manner, AUY922-induced expression of NUPR1 might confer drug resistance. Therefore, NUPR1 and Mcl-1 expression may be useful biomarkers for AUY922 response and personalized medicine for HCC.

Sorafenib is the standard treatment for patients with advanced HCC, but with only modest efficacy. As sorafenib remains the only approved drug for HCC treatment, to improve treatment outcomes, different combination therapies of sorafenib with either conventional cytotoxic chemotherapy or other targeted specific agents have been evaluated.[2] Here, we demonstrated that targeting HSP90 synergized the effect of sorafenib in a dose- and cell-type-dependent manner. Finally, the *in vivo* studies demonstrated that AUY922 treatment suppressed tumor growth and inhibited cell proliferation and angiogenesis in an HCC xenograft model.

Overall, our results provide a preclinical proof of concept for the efficacy of AUY922 in HCC treatment. AUY922 was well tolerated *in vivo* and lacks toxicity in human primary normal hepatocytes, thus supporting its potential use in HCC treatment as a single agent or in combination with sorafenib, or other molecular targeted anticancer drugs.

References

1. Forner A, Reig M, Bruix J. Hepatocellular carcinoma. *Lancet* 2018;391:1301–14.
2. Cervello M, McCubrey JA, Cusimano A, et al. Targeted therapy for hepatocellular carcinoma: novel agents on the horizon. *Oncotarget* 2012;3:236–60.
3. Llovet JM, Ricci S, Mazzaferro V, et al. Sorafenib in advanced hepatocellular carcinoma. *N Engl J Med* 2008;359:378–90.
4. Schulze K, Imbeaud S, Letouze E, et al. Exome sequencing of hepatocellular carcinomas identifies new mutational signatures and potential therapeutic targets. *Nat Genet* 2015;47:505–11.
5. Friemel J, Rechsteiner M, Frick L, et al. Intratumor heterogeneity in hepatocellular carcinoma. *Clin Cancer Res* 2015;21:1951–61.
6. Li L, Wang H. Heterogeneity of liver cancer and personalized therapy. *Cancer Lett* 2016;379:191–7.
7. Cancer Genome Atlas Research Network. Comprehensive and integrative genomic characterization of hepatocellular carcinoma. *Cell* 2017;169:1327–41.
8. Ding XX, Zhu QG, Zhang SM, et al. Precision medicine for hepatocellular carcinoma: driver mutations and targeted therapy. *Oncotarget* 2017;8:55715–30.
9. Verma S, Goyal S, Jamal S, et al. Hsp90: friends, clients and natural foes. *Biochimie* 2016;127:227–40.
10. Wang C, Zhang Y, Guo K, et al. Heat shock proteins in hepatocellular carcinoma: molecular mechanism and therapeutic potential. *Int J Cancer* 2016;138:1824–34.
11. Wu J, Liu T, Rios Z, et al. Heat shock proteins and Cancer. *Trends Pharmacol Sci* 2017;38:226–56.
12. Yang H, Lee MH, Park I, et al. HSP90 inhibitor (NVP-AUY922) enhances the anti-cancer effect of BCL-2 inhibitor (ABT-737) in small cell lung cancer expressing BCL-2. *Cancer Lett* 2017;411:19–26.
13. Park KS, Yang H, Choi J, et al. The HSP90 inhibitor, NVP-AUY922, attenuates intrinsic PI3K inhibitor resistance in KRAS-mutant non-small cell lung cancer. *Cancer Lett* 2017;406:47–53.
14. Wang CY, Guo ST, Wang JY, et al. Inhibition of HSP90 by AUY922 preferentially kills mutant KRAS Colon Cancer cells by activating Bim through ER stress. *Mol Cancer Ther* 2016;15:448–59.
15. Kosovec JE, Zaidi AH, Kelly LA, et al. Preclinical study of AUY922, a novel Hsp90 inhibitor, in the treatment of esophageal adenocarcinoma. *Ann Surg* 2016;264:297–304.
16. Akahane K, Sanda T, Mansour MR, et al. HSP90 inhibition leads to degradation of the TYK2 kinase and apoptotic cell death in T-cell acute lymphoblastic leukemia. *Leukemia* 2016;30:219–8.
17. Gao Q, Wang ZC, Duan M, et al. Cell culture system for analysis of genetic heterogeneity within hepatocellular carcinomas and response to pharmacologic agents. *Gastroenterology* 2017;152:232–42.
18. Hirschfield H, Bian CB, Higashi T, et al. In vitro modeling of hepatocellular carcinoma molecular subtypes for anti-cancer drug assessment. *Exp Mol Med* 2018;50:e419.
19. Schmidt B, Wei L, Deperalta DK, et al. Molecular subclasses of hepatocellular carcinoma predict sensitivity to fibroblast growth factor receptor inhibition. *Int J Cancer* 2016;138:1494–505.
20. Finn RS, Aleshin A, Dering J, et al. Molecular subtype and response to dasatinib, and Src/Abl small molecule kinase inhibitor, in hepatocellular carcinoma cell lines in vitro. *Hepatology* 2013;57:1838–46.
21. Fuchs BC, Fujii T, Dorfman JD, et al. Epithelial-to-mesenchymal transition and integrin-linked kinase mediate sensitivity to epidermal growth factor receptor inhibition in human hepatoma cells. *Cancer Res* 2008;68:2391–9.
22. Zhao H, Desai V, Wang J, et al. Epithelial-mesenchymal transition predicts sensitivity to the dual IGF-1R/IR inhibitor OSI-906 in hepatocellular carcinoma cell lines. *Mol Cancer Ther* 2012;11:503–13.
23. Emma MR, Iovanna JL, Bachvarov D, et al. NUPR1, a new target in liver cancer: implication in controlling cell growth, migration, invasion and sorafenib resistance. *Cell Death Dis* 2016;7:e2269.
24. Cervello M, Notarbartolo M, Landino M, et al. Downregulation of wild-type beta-catenin expression by interleukin 6 in human hepatocarcinoma HepG2 cells: a possible role in the growth-regulatory effects of the cytokine? *Eur J Cancer* 2001;37:512–9.
25. Cusimano A, Balasus D, Azzolina A, et al. Oleocanthal exerts antitumor effects on human liver and colon cancer cells through ROS generation. *Int J Oncol* 2017;51:533–44.
26. Cusimano A, Foderà D, D'Alessandro N, et al. Potentiation of the antitumor effects of both selective Cyclooxygenase-1 and Cyclooxygenase-2 inhibitors in human hepatic Cancer cells by inhibition of the MEK/ERK pathway. *Cancer Biol Ther* 2007;6:1461–8.
27. Cusimano A, Puleio R, D'Alessandro N, et al. Cytotoxic activity of the novel small molecule AKT inhibitor SC66 in hepatocellular carcinoma cells. *Oncotarget* 2015;6:1707–22.
28. Augello G, Modica M, Azzolina A, et al. Preclinical evaluation of antitumor activity of the proteasome inhibitor MLN2238 (ixazomib) in hepatocellular carcinoma cells. *Cell Death Dis* 2018;9:28.
29. Cervello M, Giannitrapani L, La Rosa M, et al. Induction of apoptosis by the proteasome inhibitor MG132 in human HCC cells: possible correlation with specific caspase-dependent cleavage of beta-catenin and inhibition of beta-catenin-mediated transactivation. *Int J Mol Med* 2004;13:741–8.
30. Cervello M, Pitarresi G, Volpe AB, et al. Nanoparticles of a polyaspartamide-based brush copolymer for modified release of sorafenib: in vitro and in vivo evaluation. *J Control Release* 2017;266:47–56.
31. Trepel J, Mollapour M, Giaccone G, et al. Targeting the dynamic HSP90 complex in cancer. *Nat Rev Cancer* 2010;10:537–49.
32. Fleischer B, Schulze-Bergkamen H, Schuchmann M, et al. Mcl-1 is an anti-apoptotic factor for human hepatocellular carcinoma. *Int J Oncol* 2006;28:25–32.
33. Siegel AB, Olsen SK, Magun A, et al. Sorafenib: where do we go from here? *Hepatology* 2010;52:360–9.

Cancer Therapy and Prevention

Cancer Therapy and Prevention

34. Cheng W, Ainiwaer A, Xiao L, et al. Role of the novel HSP90 inhibitor AUY922 in hepatocellular carcinoma: potential for therapy. *Mol Med Rep* 2015;12:2451–6.

35. Ayrault O, Godeny MD, Dillon C, et al. Inhibition of Hsp90 via 17-DMAG induces apoptosis in a p53-dependent manner to prevent medulloblastoma. *Proc Natl Acad Sci U S A* 2009;106: 17037–42.

36. Muller P, Hrstka R, Coomber D, et al. Chaperone-dependent stabilization and degradation of p53 mutants. *Oncogene* 2008;27: 3371–83.

37. Ding Z, Shi C, Jiang L, et al. Oncogenic dependency on β-catenin in liver cancer cell lines correlates with pathway activation. *Oncotarget* 2017;8:537–49.

38. Su YH, Tang WC, Cheng YW, et al. Targeting of multiple oncogenic signaling pathways by Hsp90 inhibitor alone or in combination with berberine for treatment of colorectal cancer. *BBA* 2015;1853: 226–72.

39. Chen WS, Chen CC, Chen LL, et al. Secreted heat shock protein 90α (HSP90α) induces nuclear factor-κB-mediated TCF12 protein expression to down-regulate E-cadherin and to enhance colorectal cancer cell migration and invasion. *J Biol Chem* 2013;2:9001–10.

40. Lee DH, Sung KS, Bartlett DL, et al. HSP90 inhibitor NVP-AUY922 enhances TRAIL-induced apoptosis by suppressing the JAK2-STAT3-Mcl-1 signal transduction pathway in colorectal cancer cells. *Cell Signal* 2015;27:293–305.

41. Davenport EL, Moore HE, Dunlop AS, et al. Heat shock protein inhibition is associated with activation of the unfolded protein response pathway in myeloma plasma cells. *Blood* 2007; 110:2641–9.

42. Giroux V, Malicet C, Barthet M, et al. p8 is a new target of gemcitabine in pancreatic cancer cells. *Clin Can Res* 2006;12:235–41.

43. Tang K, Zhang Z, Bai Z, et al. Enhancement of gemcitabine sensitivity in pancreatic cancer by co-regulation of dCK and p8 expression. *Oncology Rep* 2011;25:963–70.

44. Palam LR, Gore J, Craven KE, et al. Integrated stress response is critical for gemcitabine resistance in pancreatic ductal adenocarcinoma. *Cell Death Dis* 2015;6:e1913.